Journal Pre-proof

Treatment of cauliflower processing wastewater by nanofiltration and reverse osmosis in view of recycling

Céline Garnier, Wafa Guiga, Lameloise Marie-Laure, Laure Degrand, Claire Fargues

PII: S0260-8774(21)00389-7

DOI: https://doi.org/10.1016/j.jfoodeng.2021.110863

Reference: JFOE 110863

To appear in: *Journal of Food Engineering*

Received Date: 19 July 2021

Revised Date: 21 October 2021

Accepted Date: 22 October 2021

Credit author statement :

Céline GARNIER : Project administration, Methodology, Investigation, Writing-Original draft
Wafa GUIGA : Supervision, Methodology, Investigation, Writing-Original draft
Marie-Laure LAMELOISE : Funding acquisition, Investigation, Writing-Original draft
Laure DEGRAND : Investigation, Resources
Claire FARGUES : Supervision, Project administration , Investigation, Writing-Original draft

Treatment of cauliflower processing wastewater by nanofiltration and reverse osmosis in view of recycling

Céline GARNIER[1], Wafa GUIGA[1,2], Marie-Laure LAMELOISE[1], Laure DEGRAND[1,2] and Claire FARGUES[1*]

[1]Université Paris-Saclay, INRAE, AgroParisTech, UMR SayFood, 91300, Massy, France
[2]Conservatoire National des Arts et Métiers, UMR SayFood, 75003, Paris, France

*Corresponding author:

Claire Fargues, AgroParisTech, 1 avenue des Olympiades, 91744, Massy Cedex, France

claire.fargues@agroparistech.fr

Tel: +33 1 69 93 50 95

Declarations of interest : None.

Keywords

Membrane process, food industry, water reuse, effluent treatment, cauliflower, reverse osmosis

Abstract

The vegetable industry is a large consumer of drinking water. This paper investigates the possibilities of Reverse Osmosis (RO) or tight Nanofiltration (NF) for the treatment of cauliflower blanching wastewater with a view to recycling within the production unit. Ultrafiltration at 100 000 g.mol^{-1} molecular weight cut-off was necessary to decrease turbidity below 1 NTU as required before NF or RO. Three NF (DK, NF270 and SRD3) and one RO (ESPA4) membranes were tested at bench-scale in a crossflow filtration mode. Only RO allowed to reach the desired quality for a reuse purpose, with an acceptable residual COD content of 225 mg O_2.L^{-1}. The Solution-Diffusion model was validated for the transfer of glucose and fructose, for NF270, DK and ESPA4 membranes and their permeability coefficients calculated.

Highlights:

- Ultrafiltration followed by reverse osmosis allows to consider recycling of cauliflower wastewater
- ESPA4 membrane at 19 bar leads to 70 L.h^{-1}.m^{-2} permeate flux and 95% COD rejection
- Solution-diffusion model considering concentration polarization was successfully applied
- DK, NF270 and ESPA4 permeabilities for fructose and glucose were determined
- Nanofiltration with 150-300 g.mol^{-1} molecular weight cut-off is not suitable, due to the transfer of small metabolites

1. Introduction

The industries that consume a large amount of water are more and more keenly concerned by the necessity to save water resources. The food industry, including the fruit and vegetable transformation sector, is particularly concerned: according to a study of the European Commission (European, 2018), water consumption in the latter ranges from 0.5 to 15 m^3/ton of processed raw material. Reuse (recycling without treatment) and reconditioning (recycling after treatment) of these effluents thus become consequential in order to reduce the environmental impact of these industries and restore water quality to an acceptable level.

Considered as robust, flexible and "green" (Dewettinck and Le, 2011; Guiga and Lameloise, 2019), membrane processes are becoming favourite technologies for treating wastewater before recycling (Warsinger et al., 2018; Wenten and Khoiruddin, 2016) especially for the food processing industry (Meneses et al., 2017). Among them, reverse osmosis (RO) or tight nanofiltration (NF) ensure the highest water quality and have already proved valuable for wastewater reconditioning in the dairy (Bortoluzzi et al., 2017; Brião et al., 2019; Suàrez et al., 2014) and brewery industries (Braeken et al., 2004). They can provide high permeate fluxes and rejections at relatively low transmembrane pressure (*TMP*) provided several issues are considered: first, adequate pre-treatment should be implemented to bring the Silt Density Index (SDI) to below 5 and turbidity to 1 NTU (Sim et al., 2018). Second, membrane operations should be run below the critical flux to avoid irreversible fouling (Aimar et al., 2010).

The possibilities of reuse and reconditioning of wastewater in the food industry, and the development of toolboxes to evaluate the impact of these solutions are primary objectives in the French research program MINIMEAU (ANR-17-CE10-0015). A recent study on carrot peeling wastewater highlighted that high-quality water could be obtained through RO or tight NF membranes after microfiltration (MF) (Garnier et al., 2020). In the vegetable-processing industry, one plant usually transforms different vegetables, either simultaneously or successively. Consequently, the present study aimed to check the feasibility of the process developed in Garnier et al. (2020) for wastewater arising from rinsing of carrots after peeling, for treating wastewater from cauliflower blanching.

In the Drinking Water Standard, lists of parameters are to be respected for both drinking water quality and the water source from which it originates (mainly surface or groundwater), while there is no regulatory context outlining the water quality of recycled industrial wastewater. For food safety, drinking water is usually requested in the food processing industry (Casani et al., 2005). In this work, characterisation of the cauliflower blanching wastewater was made in order to select key parameters to be eliminated. Optimized pre-treatment and membrane treatment were selected with drinking water quality as the objective. Finally, the Solution-Diffusion model, commonly used to represent water and solutes transfer in non-porous membranes (Qasim et al., 2019; Wijmans and Baker, 1995) was applied to obtain water and solutes permeabilities for NF and RO membranes, considering the concentration polarization phenomenon. In this work, it was acquired especially for sugars contained in cauliflower effluent, and compared with data extracted from the literature results. Such database is essential for the design tool developed in the MINIMEAU Project.

2. Material and Methods

2.1. Wastewater origins

The wastewater was obtained from the French factory already selected by the Technical Center for Food Product Conservation (CTCPA, Paris, France) for the study of Garnier et al. (2020) on carrot processing wastewater. This factory produces several frozen vegetables sometimes on the same production line. Effluents of cauliflower processing are produced at the outlet of several operation units. In particular, a cleaning unit is used only for cauliflower and a blanching and freezing unit alternately for all vegetables (Fig. 1). Blanching consists in a short heat treatment with hot water (80 °C to 100 °C) to inactivate or delay bacterial growth and enzyme action. Cauliflower wastewater collected at the outlet of the blanching operation unit was selected for our study and stored at -18 °C before treatment tests. Drinking water used in the factory was analysed as a reference.

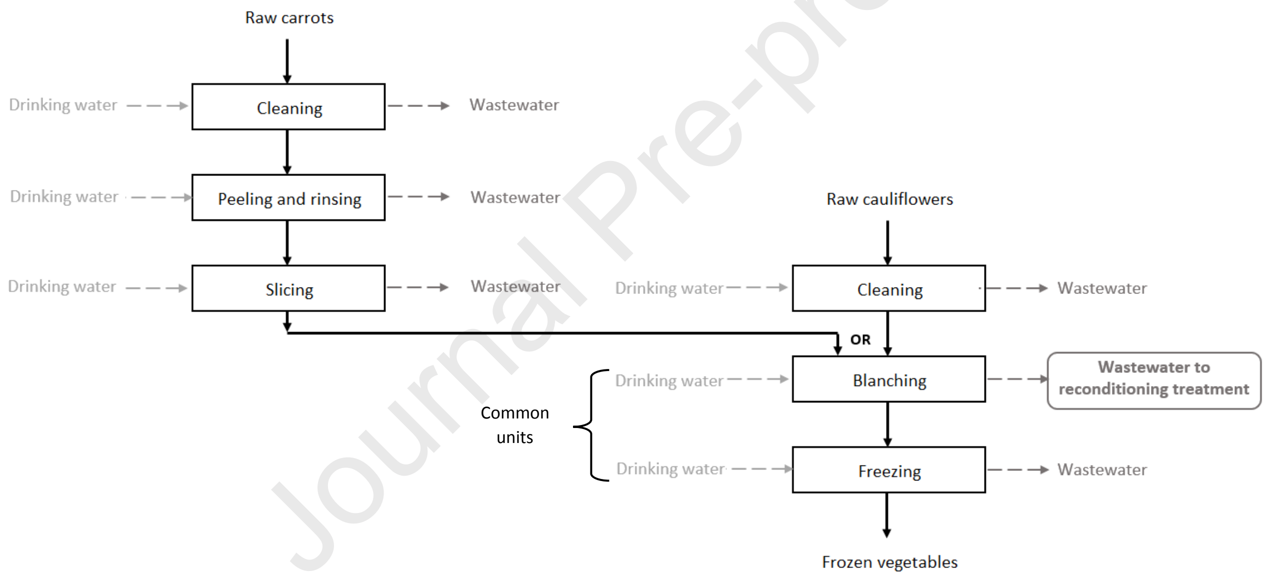

Fig. 1. Schematic representation of vegetable processing operation in the factory under study.

2.2. Analytical methods

The following analyses were performed:

- Global parameters: Total Suspended Solids (TSS), particulate and dissolved Carbon Oxygen Demand (COD), conductivity, pH, turbidity, Carbonate Hardness (CH), Total Nitrogen (TN), optical density (OD), color,
- Dissolved organic pollution: glucose, fructose (accuracy ± 4%) and sucrose (accuracy ± 5%),
- Free and total chlorine (accuracy ± 0.06 mg.L^{-1} Cl_2),
- Ionic composition: chloride, nitrite, nitrate, phosphate, sulphate, sodium, ammonium, potassium, magnesium and calcium (accuracy ± 2.5%).

Most analytical methods are already described in Garnier et al. (2020). High-performance ion-exchange chromatography (HPIC) was used to analyse anions and cations as well as sugars. At the pH of the effluent (4.7) and based on the equilibrium diagram of CO_2, the concentration of carbonate in the effluent was negligible meaning that Carbonate Hardness (CH) could represent the concentration of bicarbonate.

COD (accuracy ± 3 %), TN, CH (variable accuracy), chlorine (free and total) were determined with rapid test tubes and photometric measurement (Nanocolor vis II - Macherey Nagel, Hoerdt, France). Color and turbidity (accuracy ± 2%) were performed with the same photometric material. Color was established in the CIELAB color space adopted by the International Commission on Illumination (CIE) in 1976, where color is expressed as three values: L* (lightness from black (0) to white (100)), a* (from green to red) and b* (from blue to yellow).

COD being mainly composed of sugars, additional organic matter was quantified through a differential COD (mg $O_2.L^{-1}$) defined as:

$$COD_{diff} = COD - COD_{sugars} \quad (1)$$

Where COD_{sugars} is the COD (mg $O_2.L^{-1}$) deduced from sugar concentrations and the stoichiometry of the oxidation reaction (1g.L^{-1} of fructose and glucose corresponds to a COD of 1.066 mg $O_2.L^{-1}$ when 1 g.L^{-1} of sucrose corresponds to a COD of 1.122 mg $O_2.L^{-1}$).

UV absorbance measurement at 216.4 nm ($OD_{216.4}$) and 264.4 nm ($OD_{264.4}$) allowed evaluating the presence of amino acids or peptides. Samples were diluted ten times.

2.3. Pre-treatment

Sieving at 169 µm and 79 µm followed by dead-end MF 0.6 µm was first implemented, as in Garnier et al. (2020). The obtained turbidity remaining too high to fulfil quality requirements for further NF or RO step, the permeate obtained from MF was further ultra-filtrated. Three UF organic membranes with different Molecular Weight Cut-Off (MWCO), namely 100 000, 10 000 and 5 000 g.mol^{-1}, were tested therefore (Table 1).

2.4. NF and RO membranes

Cauliflower processing wastewater contained sucrose (MW = 342 g.mol^{-1}) and mainly glucose and fructose (MW = 180.16 g.mol^{-1}). Consequently, three NF membranes with MWCO between 150 and 300 g.mol^{-1} and one RO membrane were selected for further purification (Table 1). New membranes were stored dry at 4 °C. To remove the protective coating or storage solution, they were dipped before experiments in a 0.4 g.L^{-1} KOH solution for 2 h and then in deionized water for 24 h minimum. Prior to experiments, membranes were pre-compacted (20 bar, 15 min) in the filtration device.

Table 1

Overview of membranes characteristics according to manufacturer's data

Supplier	Membrane	Type	Rejection	MWCO ($g.mol^{-1}$)	Active layer polymer	Maximum temperature (°C)	Maximum pressure (bar)	Pure water permeability ($20°C$ - $L.h^{-1}.m^{-2}.bar^{-1}$)
Alfa Laval (Elancourt, France)	FS40PP	UF	-	100 000	Fluoro polymer	60	10	78 [a]
Koch Membrane Systems Division (Lyon, France)	HFK-131	UF	-	10 000	Polyethersulfone	55	9.7	53 [a]
Koch Membrane Systems Division (Lyon, France)	HFK-328	UF	-	5 000	Polyethersulfone	55	9.7	33 [a]
GE water & process technologies (Saint-Thibault-des-Vignes, France)	DK	NF	98% 2000 ppm $MgSO_4$ (7.6 bar, 25°C)	150–300	Semi-aromatic polypiperazine amide	50	41.4 bar if $\theta < 35$ °C; 30 bar otherwise	4.0 [b]
DOW France (Saint-Denis, France)	NF270	NF	97% 2000 ppm $MgSO_4$ (4.8 bar, 25°C)	150–300	Semi-aromatic polypiperazine amide	45	41	14.8 [b]
Koch Membrane Systems Division (Lyon, France)	SR3D	NF	> 99.0% 5000 ppm $MgSO_4$ (6.5 bar, 25°C)	200	Proprietary Thin-Film Composite polyamide	50	44.8	7.5 [b]
Hydranautics – Nitto France (Roissy, France)	ESPA4	RO	99.2% (99.0% minimum) 1500 ppm NaCl (10.3 bar, 25°C)	-	Aromatic polyamide Thin-Film Composite	45	40	6.3 [b]

([a]) This study; ([b]) from Garnier et al., 2020

2.5. Membrane setup and operating conditions

Experiments were run using the LabStak M20 filtration device from Alfa Laval described in Garnier et al. (2020). It allows testing several flat-sheet membranes simultaneously. The effective area for each membrane was 2 x 0.018 m^2.

To study water permeability and solutes' rejection, experiments were run in total recirculation mode: deionized water filtration (< 2 h) for pure water permeability measurement, wastewater filtration (< 8 h), and deionized water filtration once more (after rinsing with deionized water for 10 min minimum). For all experiments, retentate flowrate was set at 300 $L.h^{-1}$ and temperature at 20 °C. For UF membranes, two transmembrane pressures (*TMP*) were tested: 3 and 5 bar. For NF and RO membranes, *TMP* was increased from 5 to 25 bar by 5 bar steps and then decreased symmetrically. Sampling and measurements were done after at least 30 min run.

Once UF membrane selection was made, filtration was run in discontinuous mode to produce a sufficient amount of ultra-filtrated permeate: the permeate stream was collected in a distinct tank and the concentrate returned to the feed tank until reaching the desired volume reduction ratio (*VRR*):

$$VRR = \frac{V_i}{V_f} \quad (2)$$

Where V_i is the initial volume in the feed tank and V_f the final volume.

3. Filtration efficiency and solution-diffusion model application

Filtration efficiency was estimated by the permeate flux J_p ($m.s^{-1}$ or $L.h^{-1}.m^{-2}$) evolution with *TMP*, as well as by the solutes' rejections Tr_i, calculated for each solute or parameter *i* (COD, COD_{diff}, total nitrogen, OD, sugars, ions).

$$J_p = \frac{Q_p}{S} \quad (3)$$

$$Tr_i = \frac{C_{r,i} - C_{p,i}}{C_{r,i}} \quad (4)$$

Where Q_p ($m^3.s^{-1}$ or $L.h^{-1}$) is the permeate flow rate, S (m^2) is the effective membrane area and $C_{r,i}$ and $C_{p,i}$ ($mol.m^{-3}$) are the concentrations of solute *i* respectively in the retentate and in the permeate.

Experimental solute *i* flux (J_i ($mol.\ s^{-1}.m^{-2}$)) through the membrane was calculated according to:

$$J_i = C_{p,i} \times J_p \quad (5)$$

The Solution-Diffusion (SD) model is commonly used for describing the transport of non-ionic organic solutes through dense membranes such as RO and tight NF ones (Nguyen, D. et al., 2016; Qasim et al., 2019; Wijmans and Baker, 1995). For diluted solutions and in the absence of irreversible fouling, this model can be simplified to predict J_p and J_i, provided the water and solutes permeabilities are known. When concentration polarization is considered on the retentate side (Aimar et al., 2010), the following equation arises for the permeate flux:

$$J_p = A_w \times [TMP - \Delta\pi] \quad (6)$$

Where A_w (m.s^{-1}.Pa^{-1} or L.h^{-1}.m^{-2}.bar^{-1}) is the pure water permeability, $TMP = \frac{P_f+P_r}{2} - P_p$ (Pa or bar) is the transmembrane pressure (P_f, P_r and P_p are the pressures in the feed, the retentate and the permeate, respectively (bar)), and $\Delta\pi = \pi_{r\,m} - \pi_p$ (Pa or bar) is the osmotic pressure gradient between the membrane interface in the retentate (considering concentration polarization) and the permeate.

A_w could be deduced with Eq. 6 for pure water filtration experiments at different *TMP*, before and after effluent treatment on the membrane.

With the same SD model, solute *i* flux is given by:

$$J_i = B_i \times [C_{r\,m,i} - C_{p,i}] \quad (7)$$

Where B_i (m.s^{-1}) is the membrane permeability to solute *i* and $C_{r\,m,i}$ (mol.m^{-3}) is its concentration at the membrane interface in the retentate, that can be estimated through the film model theory:

$$C_{r\,m,i} = C_{p,i} + [C_{r,i} - C_{p,i}] \times exp^{\frac{Jp}{k_i}} \quad (8)$$

Where k_i (m.s^{-1}) is the mass transfer coefficient of solute *i* in the polarization layer.

To assess the simplified Solution-Diffusion model and determine k_i, and B_i, eq. (5), (7) and (8) were combined to give:

$$\ln\left(\frac{C_{p,i} \times J_p}{C_{r,i} - C_{p,i}}\right) = \ln(B_i) + \frac{J_p}{k_i} \quad (9)$$

Plotting $\ln\left(\frac{C_{p,i} \times J_p}{C_{r,i} - C_{p,i}}\right)$ *vs* J_p led to the graphical determination of B_i and k_i.

4. Results and Discussion

4.1. Characterisation of raw wastewater

Cauliflower processing wastewater had a particular odour which could be attributed to sulphur and N-bearing molecules, and foaming attested the presence of proteins. Table 2 shows the composition of the blanching wastewater (two samples). The difference between total and dissolved COD was within the accuracy limit.

Fructose and glucose represented respectively 72% and 46% of the total COD of the raw wastewater, showing its variability. These proportions increased to 99% and 79% when raw wastewater was micro filtrated, indicating that these are the main dissolved organic substances present. Other organic dissolved substances were estimated by UV spectrophotometry at 216.4 nm (possibly corresponding to peptide bonds) and 264.4 nm (corresponding to aromatic rings), as well as by TN measurement. These may be amino acids or peptides/proteins containing aromatic rings like histidine, phenylalanine, tryptophan and tyrosine, present in cauliflowers.

By comparing the composition of wastewater with that of typical cauliflower (Table 2), the transfer of sugars and most minerals (phosphate, sulphate, sodium, potassium, magnesium and calcium) into wastewater during blanching is confirmed. Glucose and fructose are transferred in the same proportion. Sucrose, present in small amounts in cauliflower (Bhandari and Kwak, 2015) is also transferred into the wastewater.

As in the study on carrot wastewater (Garnier et al., 2019; Garnier et al., 2020), TSS, COD, conductivity, fructose, glucose and sucrose were selected as key parameters. Concerning the French drinking water standard and regarding ions, only ammonium was out of the range (8–12 $mg.L^{-1}$ in raw wastewater *vs* 0.1 $mg.L^{-1}$ in French standard), so it was selected as another key parameter. The other ions were merged as key parameter "conductivity". As raw wastewater was white with an orange tint, color was also monitored.

201 **Table 2**

202 Characteristics and composition of cauliflower blanching raw wastewater (two samples from cauliflower
203 blanching), cauliflower and drinking water

Parameter	Raw wastewater	Cauliflower (USDA*)	Drinking water (French standard)	Drinking water (factory)
Temperature (°C)	50 – 80	ni	≤ 25	nd
TSS ($mg.L^{-1}$)	150 – 290	ni	-	nd
Total COD ($mg\ O_2.L^{-1}$)	7 410 – 10 120	ni	-	3.8
Dissolved COD ($mg\ O_2.L^{-1}$)	7 560 – 10 290	ni	-	nd
Total Nitrogen ($mg\ N.L^{-1}$)	190 – 265	ni	-	nd
Conductivity ($\mu S.cm^{-1}$)	2 420 – 2 640	ni	180 – 1 000	261
pH	5.8 – 5.9	ni	6.5 – 9	6.86
Turbidity (NTU)	45 – 125	ni	≤ 0.5	< 0.1
Color	L* =66 – 90 a* = 11 – 23 b*= 11 – 21	ni	Acceptable to consumers and no abnormal change	nd
UV absorbance	$OD_{216.4}$ = 2 200 – 2 360 $OD_{264.4}$ = 950 – 1 230	ni	-	nd
Carbonate hardness (°f)	24.5 – 23.5	ni	-	3.5
Fructose	2 130 – 2 210 $mg.L^{-1}$	0.97 g/100g	-	absence
Glucose	1 930 – 2 190 $mg.L^{-1}$	0.94 g/100g	-	absence
Sucrose	170 – 630 $mg.L^{-1}$	0 g/100g	-	absence
Cl^- ($mg.L^{-1}$)	110 – 140	ni	≤ 250	42
NO_2^- ($mg.L^{-1}$)	< LOD	ni	≤ 0.5	< LOD
NO_3^- ($mg.L^{-1}$)	16 – 21	ni	≤ 50	5
SO_4^{2-} ($mg.L^{-1}$)	100 – 140	ni	≤ 250	15
PO_4^{3-}	80 – 100 $mg.L^{-1}$	P: 44 g/100g	-	< LOD
Na^+	32 – 40 $mg.L^{-1}$	30 g/100g	≤ 200	19
NH_4^+ ($mg.L^{-1}$)	8 – 12	ni	≤ 0.1	< LOD
K^+	1 030 – 1 050 $mg.L^{-1}$	299 g/100g	-	4
Mg^{2+}	34 – 44 $mg.L^{-1}$	15 g/100g	-	6
Ca^{2+}	78 – 92 $mg.L^{-1}$	22 g/100g	-	22

204 * https://fdc.nal.usda.gov/fdc-app.html#/food-details/170393/nutrients published 4/1/2019. ** ni: not indicated, nd: not determined

4.2. Pre-treatment selection

The removal efficiency of the sieving-MF pre-treatment was 60% for TSS, 34% for COD, 17% for $OD_{216.4}$, 39% for $OD_{264.4}$ and null for sugars. Nevertheless, the residual turbidity (average 48 NTU) was too high for feeding a NF or RO process. Additional pre-treatment with UF membrane (MWCO of 100 000, 10 000 or 5 000 $g.mol^{-1}$) was then experienced on microfiltration permeate. Whatever the pressure (3 and 5 bar) and the membrane, the residual turbidity was below 0.5 NTU, complying with the recommendations of the NF and RO manufacturers. Membrane FS40PP with the highest MWCO (100 000 $g.mol^{-1}$) and a 3 bar pressure was preferred as it limited permeability loss during the filtration stage (41%, against 68% and 62% with membranes of 10 000 and 5 000 $g.mol^{-1}$ MWCO, respectively).

Finally, the removal efficiency of this pre-treatment (sieving + microfiltration + ultrafiltration on FS40PP at *VRR* 3.5) reached 99% for turbidity, 50% for COD, 12% for COD_{diff}, 42% for TN, 40% for conductivity, 26% for $OD_{216.4}$ and 49% for $OD_{264.4.}$ The decrease in sugar concentrations was unexpected: 56% for fructose, 98% for glucose and 100% for sucrose. This result was due to fermentation (Paramithiotis et al., 2010) during storage even if mostly at 4°C, detected by the decrease of pH and chlorine concentration, and confirmed by specific acetate and lactate peaks on HPIC chromatograms.

4.3. NF and RO performances

4.3.1. Critical flux, concentration polarization and fouling

All the following experiments were performed with pure water or with the pre-treated wastewater produced as described in section 4.2. Results are presented on Fig. 2, from which pure water permeability A_w could be deduced according to Eq. 6 (with $\Delta\pi = 0$) (Table 3). For SR3D and ESPA4 membranes, A_w values before effluent filtration were similar to those in Garnier et al (2020) (Table 1), while they appeared much lower or higher respectively for NF270 (-30%) and DK (+ 45%).

A small A_w decrease was observed after NF or RO treatment proving that fouling had occurred during effluent treatment. For wastewater filtration at the lowest *TMP* values, the relation between J_P and *TMP* was linear, showing that no fouling had yet occurred but only a reversible concentration polarization phenomenon (eq. 8) (Aimar, 2006). Above a given flux value, named the critical flux, it was no longer linear meaning that irreversible concentration polarization occurred together with a likely irreversible fouling (Aimar et al., 2010). The critical flux and corresponding pressure obtained graphically (Table 4) show that membranes do not differ from each other on these parameters but rather on A_W level (Table 3). To confirm the fouling phenomenon, J_P was studied over time and compared with initial pure water flux: for each *TMP* applied up to 15 bar, flux measurements were made after 5 min (initial flux) and 30 min; for 25 bar, it was after 5, 15 and 30 min. *TMP* was then decreased (20, 15, 10, 5 and 1 bar) and a measurement was made after 10-min run. As shown in Fig. 2, during pressure increase and below the critical flux, the steady state was quickly reached as the permeate flux was almost the same after 5 and 30 min. On the contrary, for NF270 membrane and above the critical flux, a decrease of up to 10% of J_p was observed over time (Fig. 2a). Moreover, hysteresis appeared for all membranes when *TMP* was decreased, confirming that critical flux had been exceeded and that fouling had developed (Aimar et al., 2010).

Table 3

Pure water permeability A_w before and after NF and RO treatment

Supplier	Membrane	Type	A_w measured at 20°C ($L.h^{-1}.m^{-2}.bar^{-1}$)	
			Before effluent filtration	After effluent filtration
DOW	NF270	NF	10.4 ± 0.4	8.9 ± 0.3
Koch	SR3D	NF	7.0 ± 0.2	6.4 ± 0.2
GE	DK	NF	5.8 ± 0.2	5.3 ± 0.2
Hydranautics	ESPA4	RO	6.4 ± 0.2	5.3 ± 0.2

a) b)

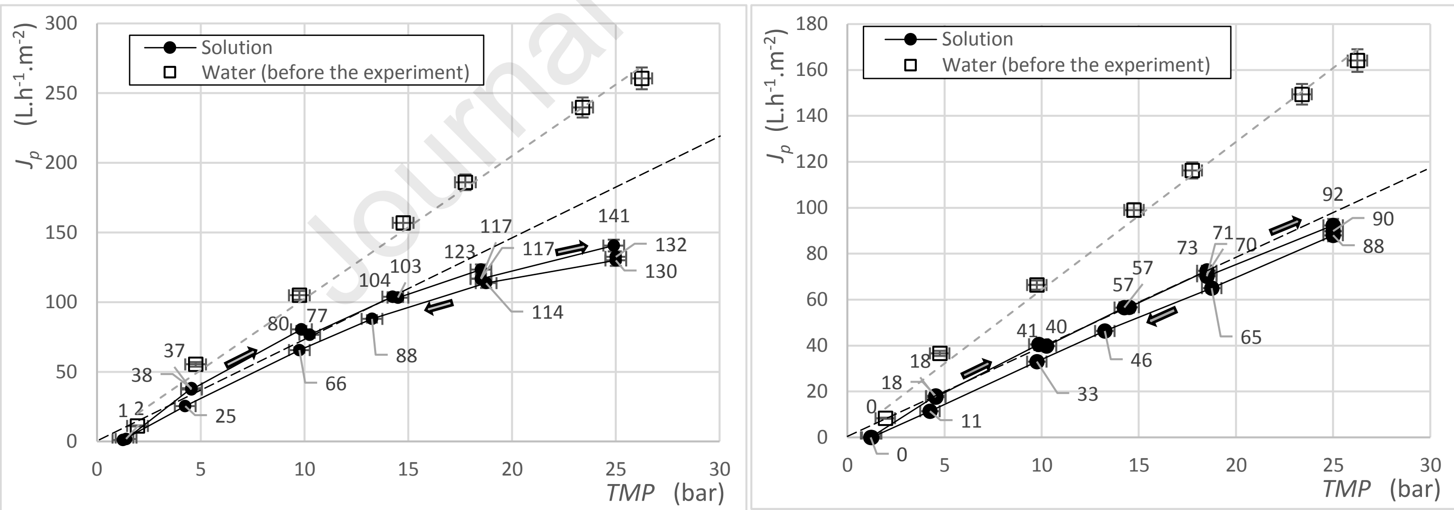

Fig. 2. Permeate flux for pure water and cauliflower pre-treated wastewater, highlighting hysteresis - J_p values obtained over time are indicated directly on the points:

(a) NF270 membrane (b) ESPA4 membrane.

Table 4

Critical flux and corresponding pressure for NF and RO membranes

Membrane	NF270	SR3D	DK	ESPA4
Critical flux ($L.h^{-1}.m^{-2}$)	100	100	90	90
Pressure at critical flux (bar)	15	18	19	24

4.3.2. Solutes rejections

The rejection performances of the membranes were compared before and after the critical flux as both concentration polarization and fouling might have a beneficial or detrimental impact on membrane selectivity (Aimar et al., 2010). Rejections of COD, glucose and fructose versus permeate flux are given Fig. 3. After pre-treatment, sucrose concentrations were below the quantification limit and were not considered. As expected, RO gave the highest rejections. For NF, rejections decreased with MWCO increase (Table 1), assessing that size exclusion was the major mechanism for NF membranes. DK and NF270 showed comparable patterns.

The COD rejections for DK (150–300 $g.mol^{-1}$), NF270 (150–300 $g.mol^{-1}$), SR3D (200 $g.mol^{-1}$) and ESPA4 (99.2% NaCl) membranes increased with *TMP* from 74.6% to 81.8%, 76.6% to 83.6%, 53.2% to 74.5% and 90.3% to 95.2%, respectively (Fig. 3-a). At 25 bar, the minimal COD values in the permeate remained high for NF (above 700 mg $O_2.L^{-1}$), and much lower for ESPA4 (208 mg $O_2.L^{-1}$). COD rejections continually increased but more and more slowly showing that exceeding the critical flux (between 90 and 100 L. $h^{-1}.m^{-2}$) is not efficient. For fructose and glucose (87–89% and 11–13% of total sugars in the retentate, respectively) the same membrane ranking was observed (Fig. 3-b). The rejections were at least 95% for NF270, 91% for DK and 98% for ESPA4 membrane which was consistent with other studies on sugars (Garnier et al., 2020; Nguyen et al., 2015). Low rejection (58 to 86%) was observed for SR3D confirming a different behaviour, as already noticed on carrot processing wastewater for protons, amino-acid-type and bicarbonates (Garnier et al., 2020). COD_{diff} rejection was always lower than the COD rejection (Fig. 3-a) which suggested that organic non-sugar molecules showed poor rejection. To investigate this, the rejections of TN, $OD_{216.4}$ and $OD_{264.4}$ were examined and compared with that for COD and COD_{diff} (Fig. 4). Results for NF270 membrane were not presented, as it behaves like DK membrane.

$OD_{216.4}$ rejections were below COD rejections for SR3D (200 $g.mol^{-1}$), similar for NF270 and DK (150–300 $g.mol^{-1}$) and above for ESPA4 membrane. This suggests that size exclusion was the main selectivity factor and that $OD_{216.4}$ represents non-aromatic and non-sugar molecules with molecular weight below 150 $g.mol^{-1}$ (Fig. 4). For ESPA4 membrane (RO), $OD_{216.4}$, $OD_{264.4}$ and TN rejections were above COD_{diff} rejection suggesting that small and undetermined molecules migrate through the membrane (Fig. 4-c). For all membranes, $OD_{264.4}$ rejections were similar and slightly above TN rejections suggesting that the main part of nitrogen compounds detected by TN measurements absorb at 264.4 nm and would thus contain aromatic amino acids identified in cauliflower (Table 5). $OD_{264.4}$ rejections of SR3D, NF270 and DK membranes were respectively between 65.0% and 80.9%, 89% and 91.7% and 87.8% and 90.1%, consistent with MW of those aromatic amino acids and MWCO of the membranes. They appeared to be better rejected by ESPA4 membrane, with $OD_{264.4}$ rejections between 96.8% and 100%. $OD_{216.4}$ rejections were always below $OD_{264.4}$ and TN rejections, showing that non-aromatic amino acids partially transfer through NF membranes, probably due to smaller MW.

a) b)

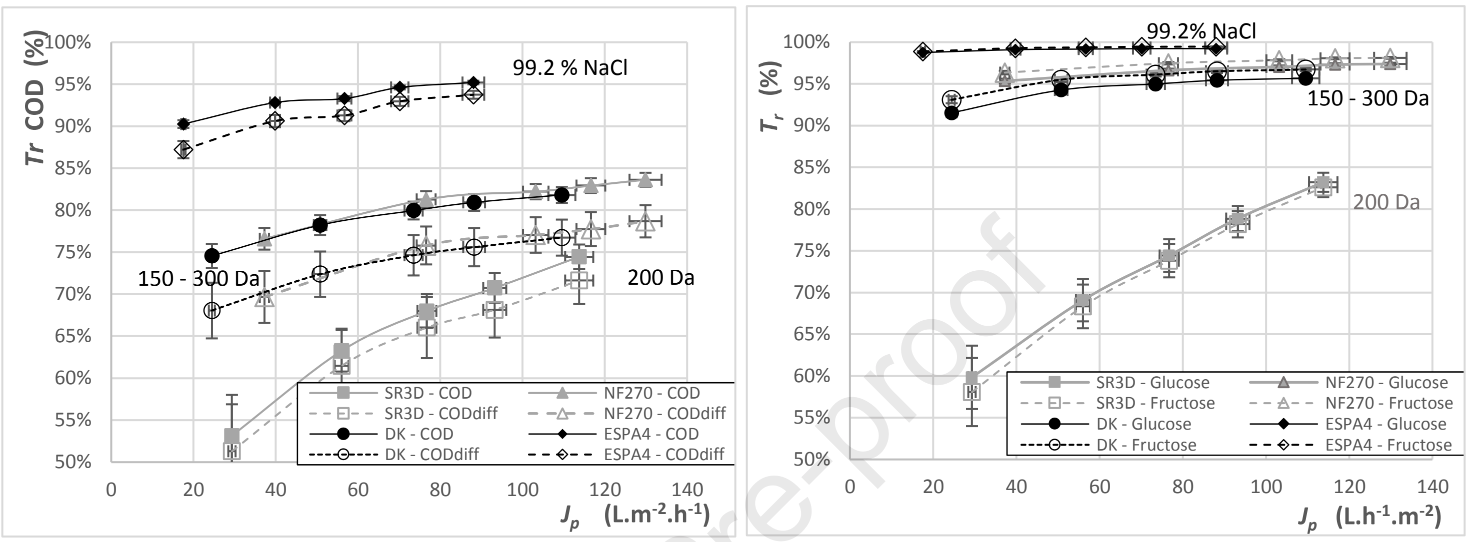

Fig. 3. COD and sugars rejection versus permeate flux (20°C, feed flow rate = 300 $L.h^{-1}$):

(a) COD and COD_{diff} (b) glucose and fructose.

Table 5

Main amino acids and aromatic amino acids in cauliflowers and their properties

Main Amino acids	Concentration in cauliflower (USDA) (g / 100 g)	Solubility in water at 25°C (g / 100 g)	Molecular weight ($g.mol^{-1}$)	Isoelectric point	Net charge at pH = 4.7
Glutamic acid	0.245	0.9	147.1	3.22	Negative
Aspartic acid	0.216	0.5	133.1	2.77	Negative
Leucine	0.107	2.4	131.2	5.98	Positive
Lysine	0.099	0.6	146.2	9.74	Positive
Alanine	0.097	16.7	89.1	6.01	Positive
Serine	0.096	25	105.1	5.68	Positive
Valine	0.092	8.8	117.1	5.96	Positive
Proline	0.079	162.5	115.1	6.30	Positive
	Aromatic amino acids (16% w/w of total amino acids in cauliflower)				
Phenylalanine	0.066	2.79	165.2	5.48	positive
Tyrosine	0.04	0.05	181.2	5.66	positive
Histidine	0.037	4.35	155.1	7.59	Positive

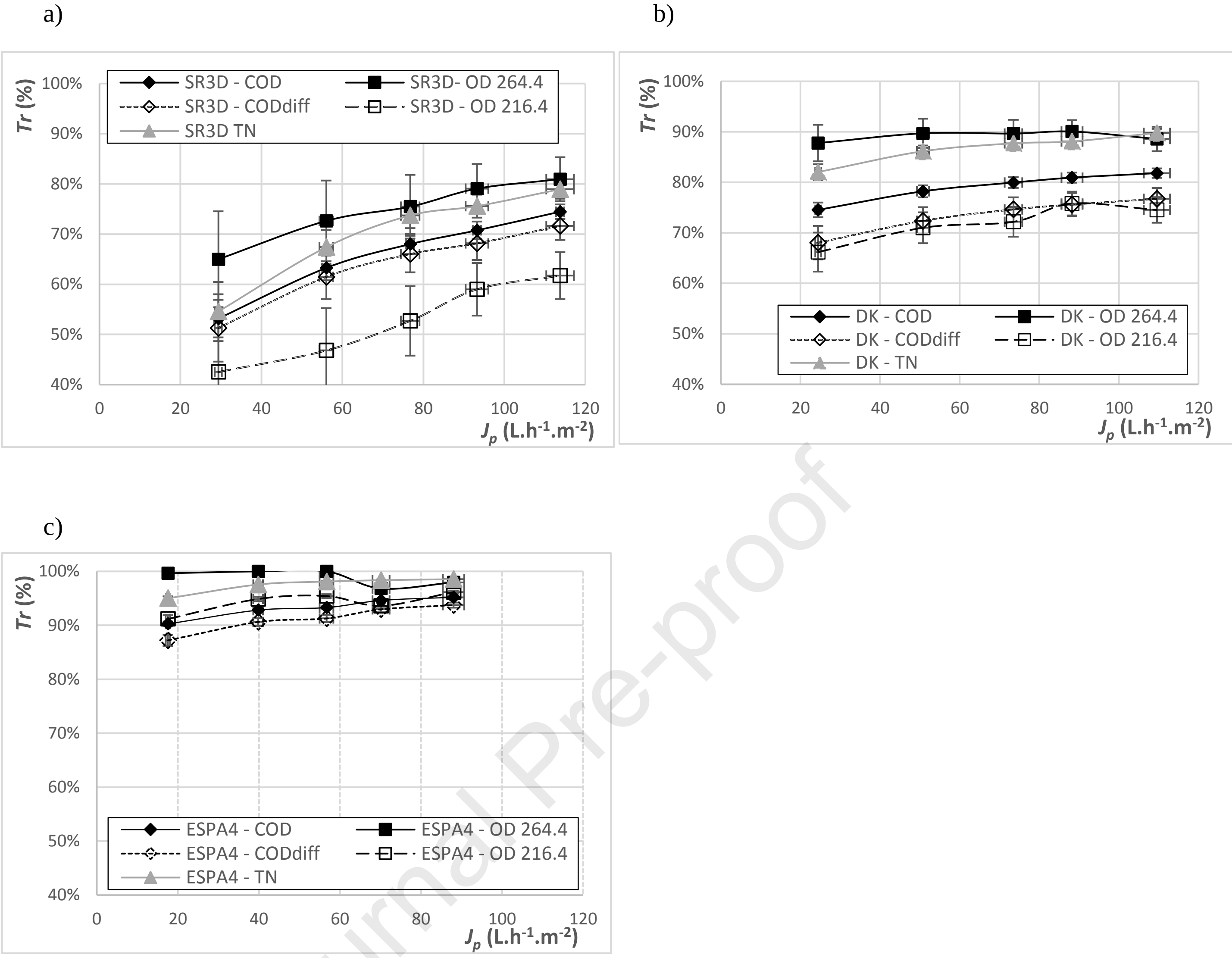

Fig. 4. COD, COD_{diff}, TN, $OD_{216.4}$ and $OD_{264.4}$ rejection versus permeate flux (20°C, feed flow rate = 300 $L.h^{-1}$): (a) SR3D membrane (b) DK membrane (c) ESPA4 membrane.

4.3.3. Minerals rejection

Rejections of sulphate and magnesium for NF270 and DK membranes were consistent with manufacturer data (Table 6). Differences can be due to operating concentrations and pressures, or to model solutions (and not complex effluents) used by manufacturers. Again, different behaviour of SR3D was observed with sulphate rejection (69.7% instead of 99%). For all minerals (Table 7), this membrane generally gave lower rejections than other NF membranes (NF270 and DK).

Table 6

Magnesium (Mg^{2+}) and sulphate (SO_4^{2-}) rejections with NF membranes à 4.6 bar

		NF270	DK	SR3D
This study	Mg^{2+} rejections	96.0 %	96.0 %	64.0 %
	SO_4^{2-} rejections	99.2 %	99.1 %	69.7 %
Manufacturer's data		97% at 4.8 bar 2 000 ppm $MgSO_4$	98% at 7.6 bar 2 000 ppm $MgSO_4$	> 99% at 6.5 bar 5 000 ppm $MgSO_4$

Ionic mass balances were established for the retentate and the permeate for DK and ESPA4 (Table 7), both at 19 bar. As in Garnier et al. (2020), for both membranes the sum of the negative charges was far lower than the positive ones, especially in the retentate and with DK. This difference can be explained by the presence of negatively charged molecules at the pH of the pre-treated effluent (pH 4.7), such as amino acids (Table 5) or organic acids (lactic acid, pKa 3.86) that were detected but not quantified in the effluent. Consequently, cations appeared globally more retained than anions in the case of the DK membrane, which can be an artifact of this proportion of negative ions not quantified in the retentate.

For DK membrane, the main identified compounds that transferred through the membranes were HCO_3^-, Cl^- and K^+. For ESPA4, the only RO membrane, it was Cl^- and K^+ (but below 5%). ESPA4 exhibited the best rejections (≥ 95%) due to its more selective polyamide layer, much thicker than that of NF membranes (Freger, 2003).

Table 7

Ionic mass balance and rejection for DK and ESPA4 membranes at 19 bar

(Note: with the Labstak pilot *Cr* is the same for both membranes)

Minerals	C_r (mmol.L^{-1})	DK		ESPA4	
		C_p (mmol.L^{-1})	*Tr* (%)	C_p (mmol.L^{-1})	*Tr* (%)
HCO_3^-	2.27	1.35	40.3	0.00	100.0
Cl^-	1.97	0.94	52.0	0.07	96.7
NO_3^-	0.15	0.09	41.7	0.02	89.3
$H_2PO_4^-$	0.49	0.02	96.9	0.00	100.0
SO_4^{2-}	0.71	0.00	100	0.00	99.8
Sum of negative charges	**6.29 meq.L^{-1}**	**2.43 meq.L^{-1}**	**61.4**	**0.08 meq.L^{-1}**	**98.7**
Na^+	0.90	0.31	65.7	0.01	99.0
NH_4^+	0.37	0.21	44.7	0.02	94.4
K^+	11.11	4.56	58.9	0.25	97.8
Mg^{2+}	0.82	0.01	98.5	0.00	99.8
Ca^{2+}	1.10	0.03	97.6	0.00	99.7
H^+	Negligible	Negligible	-	Negligible	-
Sum of positive charges	**16.21 meq.L^{-1}**	**5.15 meq.L^{-1}**	**68.2**	**0.29 meq.L^{-1}**	**98.2**
Negative charges missing	9.91 meq.L^{-1}	2.72 meq.L^{-1}		0.21 meq.L^{-1}	

Rejections of the main monovalent (Fig. 5) and divalent ions (Fig. 6) are presented separately. Due to their low concentration in the raw wastewater (Table 2), ammonium, sodium and nitrate rejections are not presented. At the pH of the effluent (4.7) and based on its equilibrium diagram, phosphate was mainly in $H_2PO_4^-$ form.

Whichever membrane was used, rejections of monovalent ions (Na^+, K^+, Cl^-, NO_3^-, HCO_3^-) were generally between 20 and 60%, much lower than that of divalent ions (Ca^{2+}, Mg^{2+}, SO_4^{2-}), above 70%. This is consistent with the Donnan space charge model (Aimar, 2006), based on electrostatic repulsions and considering the ions' valence. Moreover, for two ions with the same charge but different radii, the one having the highest charge density would exhibit the highest rejection (Epsztein et al., 2018). This may explain the highest rejection of Cl^- as compared to NO_3^-, or that of Na^+ as compared to NH_4^+, due to their respective ionic radii (Lide, 2004; Shannon, 1976). Far more $H_2PO_4^-$ is rejected due to its higher molecular weight (MW = 98 g.mol^{-1}).

ESPA4 led to the best rejections, at about 100% for divalent ions and above 95% for monovalent ones provided pressure was above 10 bar (or J_p above 40 L.h^{-1}.m^{-2}).

a)

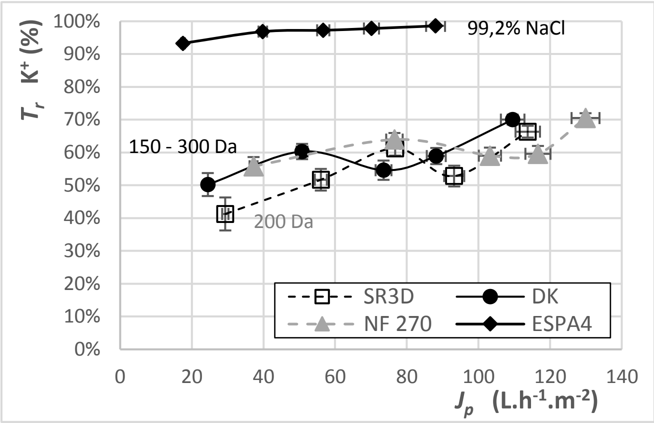

b)

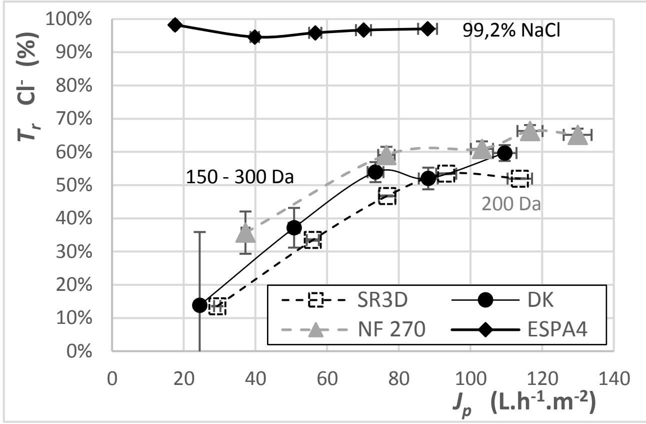

c)

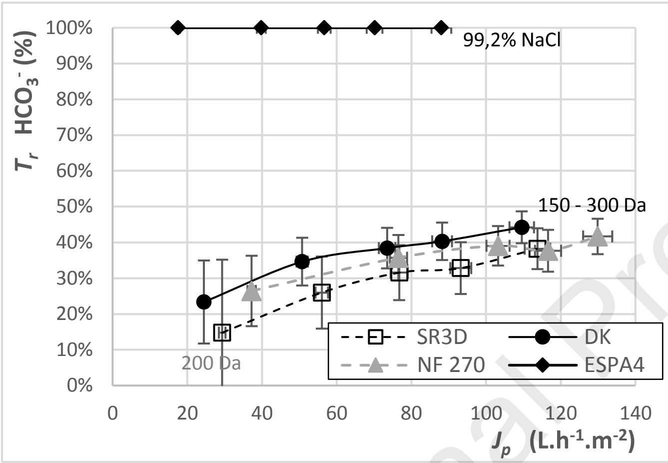

Fig. 5. Monovalent ions rejection versus permeate flux (20°C, feed flow rate = 300 L.h^{-1}):

(a) K^+ (b) Cl^- (c) HCO_3^-.

a)

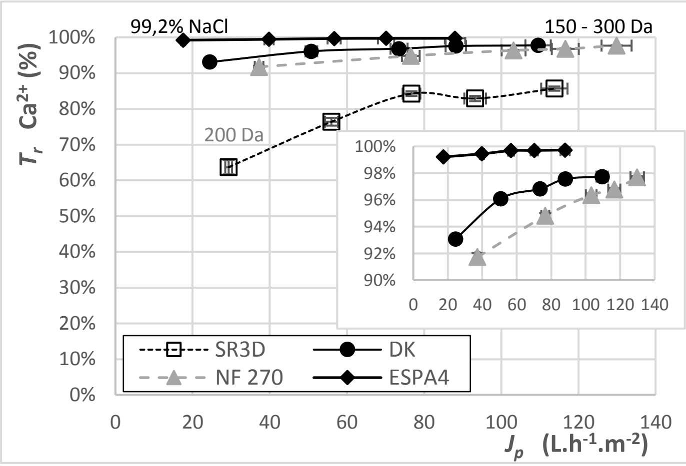

b)

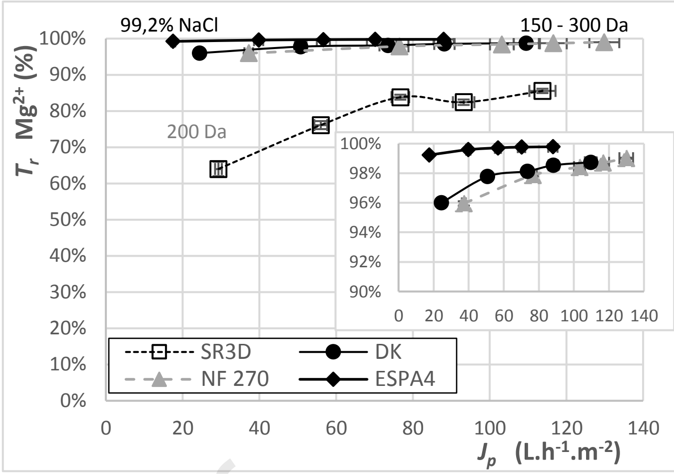

c)

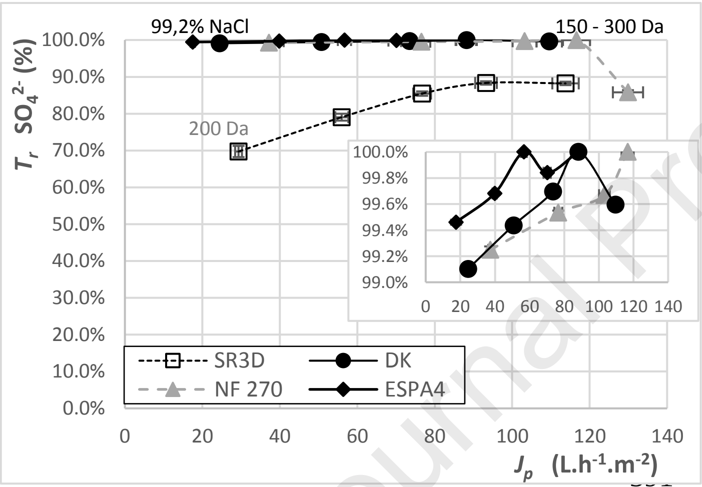

Fig. 6. Divalent ions rejection versus permeate flux (20°C, feed flow rate = 300 $L.h^{-1}$):

(a) Ca^{2+} (b) Mg^{2+} (c) SO_4^{2-}.

4.3.4 Choice of NF or RO membranes for the reconditioning treatment

Comparable results were observed with NF270 and DK membranes and lower performance (lower rejections) with SR3D membrane. NF270 at *TMP* = 15 bar and DK at *TMP* = 19 bar (pressure at critical flux) appeared as the best compromises for COD rejection and permeate flux. With RO membrane (ESPA4), the rejections were higher and critical flux corresponded to *TMP* = 24 bar (Table 4). To obtain the best compromise between COD rejection and permeate flux and to ensure a residual COD in the permeate below 400 mg $O_2.L^{-1}$, ESPA4 membrane was selected at about 19 bar. The permeate quality indicators are summarized in Table 8. For an equivalent permeate flux, the ESPA4 treatment of complex carrot peeling effluent at about 15 bar had allowed a better permeate quality (Garnier et al., 2020). This can be explained by the much lower organic load of the carrots processing wastewater (Table 9), similar rejections leading to lower concentrations in the permeate. An additional explanation may be a higher fermentation of sugar due to longer storage in the case of cauliflower processing wastewater, leading to an increase in small metabolites content such as acetic or lactic acids, which can permeate through the membrane.

Table 8

Permeate quality for selected membranes and optimized conditions

	NF270 (NF)	DK (NF)	ESPA4 (RO)
Optimum *TMP* (bar)	15	19	19
J_p ($L.h^{-1}.m^{-2}$)	103	88	70
Total COD (mg $O_2.L^{-1}$)	733	797	225
TN ($mgN.L^{-1}$)	15	17	2
Conductivity ($\mu S.cm^{-1}$)	512	527	83
pH	5.1	4.9	3.8
Carbonate Hardness (°f)	14.2	13.5	< 2
Fructose ($mg.L^{-1}$)	18	31	5
Glucose ($mg.L^{-1}$)	3	5	1
Sucrose ($mg.L^{-1}$)	< 1	< 1	< 1
Cl^- ($mg.L^{-1}$)	26	33	2
NO_3^- ($mg.L^{-1}$)	7	6	1
PO_4^{3-} ($mg.L^{-1}$)	< 1	1	< 1
SO_4^{2-} ($mg.L^{-1}$)	< 1	< 1	< 1
Na^+ ($mg.L^{-1}$)	7	7	< 1
NH_4^+ ($mg.L^{-1}$)	3	4	< 1
K^+ ($mg.L^{-1}$)	177	178	10
Mg^{2+} ($mg.L^{-1}$)	< 1	< 1	< 1
Ca^{2+} ($mg.L^{-1}$)	2	1	< 1
$OD_{216.4}$	0.445	0.404	0.106
$OD_{264.4}$	0.031	0.040	0.012
Color	L* = 100.1 a* = 0.0 b*= 0.1 (colorless)	L* = 100.0 a* = 0.0 b*= 0.1 (colorless)	L* = 100.1 a* = 0.0 b*= 0.0 (colorless)

Table 9

Rejection efficiency of RO treatment with ESPA4

	Carrot / *TMP* = 15 bar (from Garnier et al., 2020)			Cauliflower / *TMP* = 19 bar		
	Retentate	Permeate	Tr_i (%)	Retentate	Permeate	Tr_i (%)
COD (mg O_2.L^{-1})	620	12	98.0	4 179	225	94.6
Sucrose (mg.L^{-1})	305	2	99.4	2	< 0.5	> 99.5
Glucose (mg.L^{-1})	61	0.5	99.2	114	1	99.2
Fructose (mg.L^{-1})	67	0.6	99.2	889	5	99.4

4.4. Sugars' transfer modelling

For glucose and fructose with the SR3D membrane, $\ln\left(\frac{C_{p,i}\times J_p}{C_{r,i}-C_{p,i}}\right)$ *vs* J_p plot was not linear (eq. 9), demonstrating that the Solution-Diffusion model was not applicable and confirming the singularity of this membrane. On the contrary, for the DK, NF270 and ESPA4 membranes, high R^2 values (0.91 to 0.99) were obtained. k_i and B_i at 293.15 K and 300 L.h^{-1} feed flowrate obtained for sugars are summarized in Table 10 and compared with those extracted from results obtained in similar operating conditions with carrot processing wastewater (Garnier et al., 2020). For both effluents, $B_{i\ glucose}$ was similar to $B_{i\ fructose}$, at about 0.45 x10^{-6} m.s^{-1} for DK and 0.3 x 10^{-6} m.s^{-1} for NF270. As observed in Almazan (2015), concentration of sugars did not affect B_i. As expected, for dense RO membrane (ESPA4), $B_{i\ \mathrm{Glu/Fru}}$ was much lower than for NF membranes, at $B_{i\ \mathrm{Glu/Fru}}$ = 0.1 x10^{-6} m.s^{-1} for cauliflower wastewater, twice that for carrot ($B_{i\ \mathrm{Glu/Fru}}$ = 0.05 x 10^{-6} m.s^{-1}). However, it may be underlined that for this membrane, rejection was quite constant with J_p, lying between 99.0 and 99.5 %, which made inaccurate k_i and B_i determination. Other studies on glucose rejection with DK membrane allowed $B_{i\ glucose}$ parameter to be extracted (Table 11). They lie between 0.25 and 0.95 x 10^{-6} m.s^{-1}, with an average at 0.55 x 10^{-6} m.s^{-1}, consistent with the average value of 0.45 x 10^{-6} m.s^{-1} in this work, despite the diverse compositions of the studied solutions.

For NF membranes, k_i values increased with retentate concentrations. It was quite the opposite for RO membrane: respectively for fructose and glucose, 23 x 10^{-6} and 18 x 10^{-6} m.s^{-1} in cauliflower effluent with higher concentrations compared to 42 x 10^{-6} and 40 x 10^{-6} m.s^{-1} in carrot processing effluent (with lower concentrations).

For all the membranes investigated and cauliflower or carrot wastewaters, B_i was far lower than k_i ($40 < k_i/B_i < 460$) and especially for ESPA4 (k_i/B_i between 360 and 460), showing that the resistance to transfer was logically mainly due to diffusion inside the membrane, increasingly with RO membranes due to their higher density. Moreover, $C_{r\ m,i}$ / C_r ratios for glucose and fructose increased with *TMP* respectively from 1.2 to 2.9 (2.3 at 19 bar) and from 1.3 to 4.0 (3.0 at 19 bar) confirming the polarisation concentration.

Table 10

k_i and B_i for fructose and glucose from the simplified Solution-Diffusion model (eq. 9) for cauliflower (this study) and carrot wastewater (from results in Garnier et al., 2020).

Solute		Fructose		Glucose	
Vegetable of raw wastewater		Cauliflower	Carrot	Cauliflower	Carrot
Concentration range ($mg.L^{-1}$)		830 – 926	63 – 69	112 – 124	59 – 63
pH		4.8	7.5	4.8	7.5
DK	k_i ($m.s^{-1}$ x 10^{-6})	33	19	30	18
	B_i ($m.s^{-1}$ x 10^{-6})	0.42	0.45	0.52	0.42
	$\boldsymbol{k_i/B_i}$	**78**	**42**	**58**	**43**
NF270	k_i ($m.s^{-1}$ x 10^{-6})	46	12	40	12
	B_i ($m.s^{-1}$ x 10^{-6})	0.33	0.23	0.41	0.22
	$\boldsymbol{k_i/B_i}$	**139**	**52**	**98**	**55**
ESPA4	k_i ($m.s^{-1}$ x 10^{-6})	23	42	18	40
	B_i ($m.s^{-1}$ x 10^{-6})	0.05	0.10	0.05	0.09
	$\boldsymbol{k_i/B_i}$	**460**	**420**	**360**	**444**

Table 11

B_i for glucose deduced from several publications obtained with the simplified Solution-Diffusion model taking concentration polarization into account (eq. 9)

Reference		Nguyen, N. et al., 2016	Almazán et al., 2015	Lyu et al., 2016		Mohammad et al., 2010	Wang et al., 2018	Zhou et al., 2013a, b
$C_{glucose}$ ($g.L^{-1}$)		10	5-100	20	0.5	3-12	4-20	4-20
DK	B_i ($m.s^{-1}$ x 10^{-6})	0.27	0.95	0.54	0.25	0.37	0.91	0.59

5. Conclusion

A complex cauliflower processing wastewater resulting from blanching was treated using membrane processes, in order to produce water of a quality high enough to be reused inside the factory. The adopted pre-treatment consisted in a double sieving step at 169 µm and 79 µm followed by a 100 000 $g.mol^{-1}$ MWCO ultrafiltration. Its removal efficiency reached 99% for turbidity, 50% for COD and 40% for conductivity especially. At industrial scale, this pre-treatment could be replaced by a single submerged hollow fibre ultrafiltration (Nelson et al., 2007). RO treatment with ESPA4 membrane was then necessary to reach the best permeate quality. It was optimized at 19 bar, leading to a residual COD value in the permeate of 225 mg $O_2.L^{-1}$ due to the transfer of small non-aromatic compounds. Solution-Diffusion model and film model theory were applicable to describe glucose and fructose transfer, for DK, NF270 and ESPA4 membranes. Permeability coefficient B_i obtained for glucose and fructose was similar (0.45 x 10^{-6} $m.s^{-1}$) and consistent with values calculated from other studies (0.25 to 0.95 x 10^{-6} $m.s^{-1}$) regardless of the concentration of glucose in the feed solution and its composition.

These results, if industrially confirmed, open the possibility of water recycling of cauliflower blanching wastewater. However, it would be necessary to investigate long-term accumulation of the residual solutes in the recycled effluent. A Life Cycle Assessment on the plant under study confirmed that this wastewater recycling through UF plus RO treatment was beneficial. It offers a way to limit the reliance on water resource and to face water restrictions that in certain regions lead to stop or delay food plants production.

Nomenclature and units

A_w	membrane permeability to pure water ($m.s^{-1}.Pa^{-1}$ or $L.h^{-1}.m^{-2}.bar^{-1}$)
B_i	membrane permeability to solute *i* ($m.s^{-1}$)
$C_{p,i}$, $C_{r,i}$, $C_{r\,m,i}$	concentration of solute i in the permeate, the retentate and at the membrane interface in the retentate, respectively ($mol.m^{-3}$)
CH	Carbonate Hardness (°f)
COD	Carbon Oxygen Demand (mg $O_2.L^{-1}$)
COD_{diff}	differential COD = difference between COD and COD_{sugars}
COD_{sugars}	COD deduced from sugar concentrations (mg $O_2.L^{-1}$)
$\Delta\pi$	osmotic pressure gradient between the membrane interface in the retentate and the permeate (Pa or bar)
J_i	flux of solute i through the membrane (mol. $s^{-1}.m^{-2}$)
J_p	permeate flux ($m.s^{-1}$, usually expressed in $L.h^{-1}.m^{-2}$)

k_i mass transfer coefficient of solute *i* in the polarization layer ($m.s^{-1}$)

OD Optical Density (-)

P_f, P_r, P_p pressure in the feed, the retentate and the permeate, respectively (Pa or bar)

$\boldsymbol{\pi_p}, \boldsymbol{\pi_{r\,m}}$ osmotic pressure in the permeate and at the membrane interface in the retentate, respectively (Pa or bar)

Q_p permeate flow rate ($m^3.s^{-1}$ or $L.h^{-1}$)

S effective membrane area (m^2)

TMP TransMembrane Pressure (Pa or bar)

TN Total Nitrogen (mg $N.L^{-1}$)

Tr_i rejection rate of solute *i* (-)

TSS Total Suspended Solids ($mg.L^{-1}$)

V_i, V_f initial and final volume of solution in the feed tank for a discontinuous filtration run (m^3)

VRR Volume Reduction Ratio (-)

Acknowledgements

This research was supported by the French National Agency for Research (ANR) through the MINIMEAU Project (ANR-17-CE10-0015). Authors thank Janaina Oliveira da Silva for her valuable contribution to this work. Technical Center for Food Product Conservation (CTCPA, Paris, France) is acknowledged for sharing its expertise in vegetable industries and for providing the industrial partner for effluent supply.

References

Aimar, P. (2006). Filtration membranaire (OI, NF, UF) Mise en œuvre et performances. *Techniques de l'ingénieur Procédés de traitement des eaux potables, industrielles et urbaines* base documentaire : TIB318DUO(ref. article : w4110).

Aimar, P., Bacchin, P., & Maurel, A. (2010). Filtration membranaire (OI, NF, UF, MFT) Aspects théoriques : perméabilité et sélectivité. *Techniques de l'ingénieur Opérations unitaires : techniques séparatives sur membranes* base documentaire : TIB331DUO(ref. article : j2790).

Almazán, J.E., Romero-Dondiz, E.M., Rajal, V.B., & Castro-Vidaurre, E.F. (2015). Nanofiltration of glucose: Analysis of parameters and membrane characterization. *Chemical engineering research and design* 94, 485-493.

Bhandari, S.R., & Kwak, J.-H. (2015). Chemical composition and antioxidant activity in different tissues of Brassica vegetables. *Molecules* 20(1), 1228-1243.

Bortoluzzi, A.C., Faitão, J.A., Di Luccio, M., Dallago, R.M., Steffens, J., Zabot, G.L., & Tres, M.V. (2017). Dairy wastewater treatment using integrated membrane systems. *Journal of environmental chemical engineering* 5(5), 4819-4827.

Braeken, L., Van der Bruggen, B., & Vandecasteele, C. (2004). Regeneration of brewery waste water using nanofiltration. *Water Research* 38(13), 3075-3082. https://doi.org/ 10.1016/j.watres..2004.03.028.

Brião, V.B., Salla, A.C.V., Miorando, T., Hemkemeier, M., & Favaretto, D.P.C. (2019). Water recovery from dairy rinse water by reverse osmosis: Giving value to water and milk solids. *Resources, Conservation and Recycling* 140, 313-323.

Casani, S., Rouhany, M., & Knochel, S. (2005). A discussion paper on challenges and limitations to water reuse and hygiene in the food industry. *Water Research* 39(6), 1134-1146. https://doi.org/ 10.1016/j.watres.2004.12.015.

Dewettinck, K., & Le, T.T. (2011). *Membrane separations in food processing*. Cambridge, The Royal Society of Chemistry.

Epsztein, R., Shaulsky, E., Dizge, N., Warsinger, D.M., & Elimelech, M. (2018). Role of ionic charge density in donnan exclusion of monovalent anions by nanofiltration. *Environmental science & technology* 52(7), 4108-4116.

European, C. (2018). *Best Available Technique (BAT) - Reference document in the food, drink and milk industries*.

Freger, V. (2003). Nanoscale heterogeneity of polyamide membranes formed by interfacial polymerization. *Langmuir* 19(11), 4791-4797.

Garnier, C., Guiga, W., Lameloise, M.-L., Degrand, L., & Fargues, C., 2019. Tools development for water recycling. 9th IWA Membrane Technology Conference (Toulouse), Poster.

Garnier, C., Guiga, W., Lameloise, M.-L., Degrand, L., & Fargues, C. (2020). Toward the reduction of water consumption in the vegetable-processing industry through membrane technology: case study of a carrot-processing plant. *Environmental Science and Pollution Research*, 1-19.

Guiga, W., & Lameloise, M.-L. (2019). Membrane separation in food processing. *Green Food Processing Techniques* (pp. 245-287). Elsevier.

Lide, D.R. (2004). *CRC handbook of chemistry and physics*. CRC press.

Lyu, H., Fang, Y., Ren, S., Chen, K., Luo, G., Zhang, S., & Chen, J. (2016). Monophenols separation from monosaccharides and acids by two-stage nanofiltration and reverse osmosis in hydrothermal liquefaction hydrolysates. *Journal of Membrane Science* 504, 141-152.

Meneses, Y.E., Stratton, J., & Flores, R.A. (2017). Water reconditioning and reuse in the food processing industry: Current situation and challenges. *Trends in Food Science & Technology* 61, 72-79. https://doi.org/ 10.1016/j.tifs.2016.12.008.

Mohammad, A.W., Basha, R.K., & Leo, C. (2010). Nanofiltration of glucose solution containing salts: Effects of membrane characteristics, organic component and salts on retention. *Journal of Food Engineering* 97(4), 510-518.

Nelson, H., Singh, R., Toledo, R., & Singh, N. (2007). The use of a submerged microfiltration system for regeneration and reuse of wastewater in a fresh-cut vegetable operation. *Separation Science and Technology* 42(11), 2473-2481. https://doi.org/ 10.1080/01496390701477147.

Nguyen, D., Lameloise, M.-L., Guiga, W., Lewandowski, R., Bouix, M., & Fargues, C. (2016). Optimization and modeling of diananofiltration process for the detoxification of ligno-cellulosic hydrolysates-study at pre-industrial scale. *Journal of Membrane Science* 512, 111-121.

Nguyen, N., Fargues, C., Guiga, W., & Lameloise, M.-L. (2015). Assessing nanofiltration and reverse osmosis for the detoxification of lignocellulosic hydrolysates. *Journal of Membrane Science* 487, 40-50.

Nguyen, N., Lameloise, M.-L., Guiga, W., Lewandowski, R., Bouix, M., & Fargues, C. (2016). Optimization and modeling of diananofiltration process for the detoxification of ligno-cellulosic hydrolysates-study at pre-industrial scale. *Journal of Membrane Science* 512, 111-121.

Paramithiotis, S., Hondrodimou, O.L., & Drosinos, E.H. (2010). Development of the microbial community during spontaneous cauliflower fermentation. *Food Research International* 43(4), 1098-1103.

Qasim, M., Badrelzaman, M., Darwish, N.N., Darwish, N.A., & Hilal, N. (2019). Reverse osmosis desalination: A state-of-the-art review. *Desalination* 459, 59-104.

Shannon, R.D. (1976). Revised effective ionic radii and systematic studies of interatomic distances in halides and chalcogenides. *Acta crystallographica section A: crystal physics, diffraction, theoretical and general crystallography* 32(5), 751-767.

Sim, L.N., Chong, T.H., Taheri, A.H., Sim, S., Lai, L., Krantz, W.B., & Fane, A.G. (2018). A review of fouling indices and monitoring techniques for reverse osmosis. *Desalination* 434, 169-188.

Suàrez, A., Fidalgo, T., & Riera, F.A. (2014). Recovery of dairy industry wastewaters by reverse osmosis. Production of boiler water. *Separation and Purification Technology* 133, 204-211. https://doi.org/ 10.1016/j.seppur.2014.06.041.

Wang, T., Meng, Y., Qin, Y., Feng, W., & Wang, C. (2018). Removal of furfural and HMF from monosaccharides by nanofiltration and reverse osmosis membranes. *Journal of the Energy Institute* 91(3), 473-480.

Warsinger, D.M., Chakraborty, S., Tow, E.W., Plumlee, M.H., Bellona, C., Loutatidou, S., Karimi, L., Mikelonis, A.M., Achilli, A., & Ghassemi, A. (2018). A review of polymeric membranes and processes for potable water reuse. *Progress in polymer science* 81, 209-237.

Wenten, I.G., & Khoiruddin (2016). Reverse osmosis applications: Prospect and challenges. *Desalination* 391, 112-125. https://doi.org/ 10.1016/j.desal.2015.12.011.

Wijmans, J.G., & Baker, R.W. (1995). The solution-diffusion model: a review. *Journal of membrane science* 107(1-2), 1-21.

Zhou, F., Wang, C., & Wei, J. (2013a). Separation of acetic acid from monosaccharides by NF and RO membranes: Performance comparison. *Journal of membrane science* 429, 243-251.

Zhou, F., Wang, C., & Wei, J. (2013b). Simultaneous acetic acid separation and monosaccharide concentration by reverse osmosis. *Bioresource technology* 131, 349-356.

Declarations of interest: none.

I, Claire Fargues and my co-authors Céline Garnier, Wafa Guiga, Marie-Laure Lameloise and Laure Degrand have no competing interests to declare.

Massy, the 15th July 2021